

RESEARCH ARTICLE

Preferred gait and walk–run transition speeds in ostriches measured using GPS-IMU sensors

Monica A. Daley[§], Anthony J. Channon^{*}, Grant S. Nolan[‡] and Jade Hall

ABSTRACT

The ostrich (*Struthio camelus*) is widely appreciated as a fast and agile bipedal athlete, and is a useful comparative bipedal model for human locomotion. Here, we used GPS-IMU sensors to measure naturally selected gait dynamics of ostriches roaming freely over a wide range of speeds in an open field and developed a quantitative method for distinguishing walking and running using accelerometry. We compared freely selected gait–speed distributions with previous laboratory measures of gait dynamics and energetics. We also measured the walk–run and run–walk transition speeds and compared them with those reported for humans. We found that ostriches prefer to walk remarkably slowly, with a narrow walking speed distribution consistent with minimizing cost of transport (CoT) according to a rigid-legged walking model. The dimensionless speeds of the walk–run and run–walk transitions are slower than those observed in humans. Unlike humans, ostriches transition to a run well below the mechanical limit necessitating an aerial phase, as predicted by a compass-gait walking model. When running, ostriches use a broad speed distribution, consistent with previous observations that ostriches are relatively economical runners and have a flat curve for CoT against speed. In contrast, horses exhibit U-shaped curves for CoT against speed, with a narrow speed range within each gait for minimizing CoT. Overall, the gait dynamics of ostriches moving freely over natural terrain are consistent with previous lab-based measures of locomotion. Nonetheless, ostriches, like humans, exhibit a gait-transition hysteresis that is not explained by steady-state locomotor dynamics and energetics. Further study is required to understand the dynamics of gait transitions.

KEY WORDS: Biped, *Struthio camelus*, Locomotion, Biomechanics, Energetics, Gait transition

INTRODUCTION

Animals use different gaits depending on the speed of movement – striding bipeds walk at slow speeds and run at higher speeds. In walking, the body vaults over relatively rigid legs, such that kinetic energy (E_k) and gravitational potential energy (E_g) fluctuate out of phase (Cavagna et al., 1977; Usherwood, 2005). In running, the body bounces on a relatively compliant leg, approximating a spring-loaded inverted pendulum, in which E_k and E_g fluctuate in phase and elastic energy is cycled in musculoskeletal tissues (Cavagna

et al., 1977; Alexander, 1992). Recent studies have demonstrated that both walking and running gaits emerge from a spring-loaded inverted pendulum (SLIP) model, with distinct gait dynamics occurring with different combinations of kinetic energy, leg compliance and leg contact conditions, resulting in different modes of oscillation (Geyer et al., 2006; S. M. O'Connor, The relative roles of dynamics and control in bipedal locomotion, PhD thesis, University of Michigan, 2009). Humans exhibit a clear and abrupt transition between distinct walking and running gaits; in contrast, ground birds, including ostriches, show more complex gait dynamics, with 'grounded running' at intermediate speeds, in which the body mechanics resemble a run, but duty factor remains above 0.5, meaning that there is no aerial phase (Gatesy and Biewener, 1991; Alexander, 2004; Rubenson et al., 2004). Nonetheless, grounded running emerges from the SLIP model within a specific range of leg stiffness, and smoothly transitions to aerial running with increasing speed (S. M. O'Connor, The relative roles of dynamics and control in bipedal locomotion, PhD thesis, University of Michigan, 2009). Thus, the steady bipedal gaits of birds and humans can be described by the same reduced-order SLIP template model.

There is long-standing interest in the factors that drive gait selection in terrestrial locomotion. The most widely accepted explanation is that animals move using gait–speed combinations that minimize the metabolic cost of transport (CoT). Classic work by Hoyt and Taylor (1981) demonstrated that horses exhibit U-shaped curves for metabolic CoT against speed, with a narrow optimum speed range for minimizing CoT within each gait. Horses also naturally prefer to use the energetically optimal speed range within each gait (Hoyt and Taylor, 1981). This classic work and subsequent experimental and modelling studies (Rubenson et al., 2004; Watson et al., 2011; Srinivasan and Ruina, 2006; Srinivasan, 2011; Usherwood and Hubel, 2012) have supported the hypothesis that gait dynamics and gait selection are driven by energy optimality.

Remarkably little is known about how animals self-select gait during natural overground locomotor behaviour. Gait dynamics and energetics have typically been measured at constant speeds on a treadmill (e.g. Hoyt and Taylor, 1981; Gatesy and Biewener, 1991; Rubenson et al., 2004; Watson et al., 2011; Smith and Wilson, 2013). Treadmills allow controlled measurement of steady gait at a speed determined by the experimenter. However, natural conditions rarely require movement with constant steady speed, and many factors can influence speed and gait selection, including varied terrain conditions and the need to move quickly just long enough to catch prey or avoid predators. Furthermore, animals can dynamically vary speed and gait to achieve average speeds between energetic optima. Thus, it remains unclear whether the notion of 'preferred' steady speeds driven by energetic optimality has widespread relevance to animals moving in more natural settings.

Structure and Motion Lab, Royal Veterinary College, Hawkshead Lane, Hatfield AL97TA, UK.

^{*}Present address: BAE Systems Applied Intelligence, Surrey Research Park, Guildford, Surrey GU2 7RQ, UK. [‡]Present address: St George's, University of London, Cranmer Terrace, London SW17 0RE, UK.

[§]Author for correspondence (mdaley@rvc.ac.uk)

 M.A.D., 0000-0001-8584-2052

Received 28 April 2016; Accepted 8 August 2016

Our limited understanding of self-selected gait characteristics of freely moving animals stems, in part, from the challenge of measuring gait dynamics in more natural conditions, such as field studies. However, recent advances in global-positioning system–inertial measurement unit (GPS-IMU) sensing loggers provide a promising new tool for understanding animal locomotor dynamics and behaviour over a broad range of conditions, including long-term field studies and predator–prey interactions (e.g. Wilson et al., 2013; Hubel et al., 2016). The goals of the current study were to (1) develop quantitative methods for measuring detailed bipedal gait dynamics using GPS-IMU sensors and (2) use these methods to measure self-selected gait–speed distributions and walk–run transition speeds in freely moving ostriches in a field-laboratory setting.

The ostrich (*Struthio camelus*) is the largest extant bird and is widely appreciated as a fast and agile bipedal athlete. Consequently, the ostrich has served as an important animal model for understanding bipedal gait dynamics and energetics (Fedak and Seeherman, 1979; Alexander et al., 1979; Abourachid and Renous, 2000; Rubenson et al., 2004; Smith et al., 2010; Watson et al., 2011; Smith and Wilson, 2013), and as an inspiration for the design of legged robots (Andrada et al., 2012; Cotton et al., 2012). Here, we measured self-selected gait dynamics of ostriches roaming in a 165×120 m grassy paddock over a wide range of speeds using GPS-IMU sensors, and compared freely selected gait–speed distributions with those reported previously from standard biomechanics laboratory measures.

MATERIALS AND METHODS

Study animals

Seven female African ostriches (*Struthio camelus* Linnaeus 1758) were hand raised from 6 weeks until reaching adult body size. At the time of the experiments, the ostriches were 18 months old, with a body mass of 112.6±8.1 kg (mean±s.d.) and standing hip height 1.26±0.04 m. The ostriches were housed as a flock in a 165×120 m paddock, with food and water available at all times. Trained handlers engaged the ostriches in daily exercise and enrichment activities; for example, by moving food and interesting objects to different locations throughout the paddock. The animals were regularly monitored by veterinary surgeons. Experiments were recorded in the home paddock. The animal handling and experimental protocols were approved by the Royal Veterinary College Ethics and Welfare Committee under the project reference number URN 2012 1138.

Data collection

The ostriches were fitted with a back-mounted GPS-IMU (3rd generation RVC GPS and inertial sensing loggers). Doppler and pseudo-range GPS data were sampled at 5 Hz. The IMU tri-axial accelerometers (±12 g) and tri-axial gyroscopes (±2000 deg s⁻¹) were recorded at 300 Hz with 12-bit precision. A static GPS base station (NovAtel, Inc., Calgary, AB, Canada) was placed on the top of a nearby building. GPS data were post-processed using commercially available software (Waypoint GrafNav version 8.10, NovAtel, Inc.), which uses L1 Doppler used to determine velocity and pseudo-range measurements to determine position. At the beginning of the recording day, all loggers were turned on and placed in a strong plastic box that was harnessed securely to the back of the ostrich using thick nylon straps and Vetwrap cohesive bandage (3M, St Paul, MN, USA). The logger was aligned with the approximate position of the body centre of mass (CoM) in the dorsal plane, with the horizontal axes aligned to fore–aft and medio-lateral

movement. By necessity, however, the vertical position of the logger was above the true body CoM. The harness and logger box together weighed less than 0.5% of body mass, and the ostriches displayed no signs of discomfort or irritation. All birds were fitted with a harness and then released into the paddock.

Data were collected for 2.5 h around midday on a single recording day, during which time the birds roamed freely in their home paddock. Data were collected on a day with clear weather and minimal cloud cover to maximize GPS signal quality, and the temperature during recording was 9–10°C. For a period of approximately 24 min within the 2.5 h period (starting from around minute 29; Fig. S1), the birds were chased in short bouts with a quad bike to motivate them to run near maximal speeds. To minimize stress and fatigue, chasers did not approach closer than 20 m, and rest periods were allowed between chase bouts. Human interaction was otherwise minimized during recording. Fig. S1 shows the distribution of the recorded data within the paddock (Fig. S1A) and the velocity of the locomotor bouts over the recording period (Fig. S1B). Outside the period of quad-bike chasing, maximum speeds were lower, but the ostriches exhibited intermittent locomotor bouts throughout the recording session (Fig. S1B).

Data processing and gait measurement

Data were analysed in SI units and then converted to normalized quantities based on gravity and effective leg length, measured as standing hip height. IMU data were filtered using a 6th order zero phase shift Butterworth bandpass filter with cut-off frequencies of 0.835 and 14.19 Hz. These cut-off frequencies were selected to be 0.5× the lowest and 2.5× the highest previously reported step frequencies for ostrich locomotion (Rubenson et al., 2004). Speed was calculated as the vector magnitude of GPS velocity plus the IMU velocity fluctuations. Bouts of locomotion were detected from the GPS velocity, based on detecting motion above a threshold speed of 0.6 m s⁻¹ and lasting at least 5.5 s. Within locomotor bouts, bandpass-filtered acceleration data were integrated once to calculate fluctuations in velocity and again to calculate displacement. Signals were visually assessed to ensure that the filtered, integrated data did not show evidence of drift, with fluctuations centred at zero (typical data shown in Fig. 1). Step cycles were detected from peaks in fore–aft velocity. For all steps within a locomotor bout, the step period was calculated as the time between subsequent fore–aft velocity peaks, speed was taken as the average over the step period, and step length was calculated by multiplying average speed by step period. Relative speed (V) was calculated as $V = \text{velocity} / \sqrt{gL}$, where L is leg length, measured as standing hip height, and g is acceleration due to gravity.

Examination of the acceleration and displacement signals revealed an abrupt shift in the signal characteristics between low and high speeds (Fig. 1). At low speeds, fore–aft oscillations were larger than vertical oscillations. As speed increased, fore–aft oscillations abruptly decreased and, simultaneously, vertical oscillations abruptly increased. We verified this pattern in the relative amplitude of fore–aft and vertical oscillations from lab-based measures, which showed relatively higher fore–aft displacements and the characteristic M-shaped ground reaction force during walking versus relatively higher vertical displacements, higher peak vertical forces and the characteristic ‘half-sine’ force trace during running (Fig. 2). Based on these observations, we detected walking, running, walk–run transitions and run–walk transitions by comparing the relative magnitude of fore–aft and vertical displacement oscillations. A continuous gait

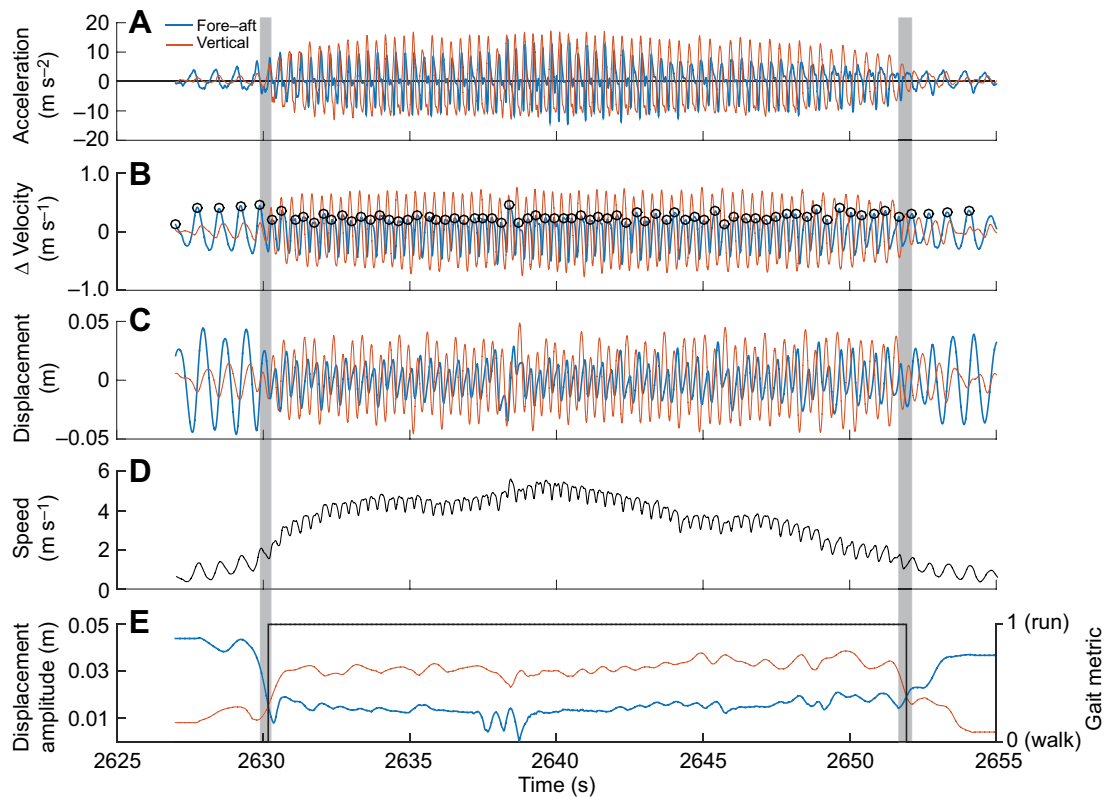


Fig. 1. Example GPS-IMU data from a representative ostrich locomotor bout that includes walking, running and walk–run and run–walk transitions. Fore–aft and vertical acceleration signals (A) were integrated once to calculate velocity fluctuations (B), and again to calculate displacement fluctuations (C). Steps were determined between successive peaks in fore–aft velocity, indicated by circles in B. Velocity fluctuations were added to the GPS velocity to calculate total speed (D). Gait (walk, run) was identified based on the relative magnitude of the fore–aft and vertical displacements (E) – the right axis in E shows fore–aft and vertical displacement amplitude derived from a continuous sine fit to the curves in C (see Materials and methods). A continuous gait metric (black line in E) was derived from Boolean comparison of vertical and fore–aft displacement. The vertical grey bars indicate the specific steps identified as walk–run and run–walk transitions, based on the intersection of the red and blue lines in E.

metric was generated by taking the amplitude of a sine fit to the displacement signals at each time point, with the fit at each time weighted by a full Hanning window equal to $4\times$ the mean step period. The sine fit window was selected to provide a smooth estimate of displacement amplitude over time that was robust to stride-to-stride variance (for example, due to balance adjustments in rough terrain). The continuous gait metric (Fig. 1E) was derived from Boolean evaluation of vertical displacement $>$ fore–aft displacement, with false (0) = walk and true (1) = run. Steps were identified as (1) ‘walk’ if fore–aft displacement amplitude was larger than vertical throughout the step, (2) ‘run’ if vertical displacement was larger than fore–aft throughout the step, (3) ‘walk–run’ transition if the gait metric shifted from walk to run within the step, and (4) ‘run–walk’ transition if the gait metric shifted from run to walk within the step (Fig. 1). This gait heuristic was consistent across individuals, robust to moderately unsteady gait, and did not require hand-tuning of parameters.

We calculated the relative energy phase for each step cycle based on the time lag and sign of the maximum cross-correlation between E_g and kinetic energy E_k , yielding a value of 0 deg for perfectly in-phase energy fluctuations and 180 deg for out-of-phase fluctuations. A gait metric could be generated based on the relative energy phase. However, we found higher stride-to-stride variance in energy phase with unsteady gait. This is consistent with previous findings that mechanical energy fluctuations vary considerably in unsteady gait, but ground reaction force magnitude remains consistent (Birn-

Jeffery and Daley, 2012; Birn-Jeffery et al., 2014), constrained by the requirements to support body weight while avoiding injurious loads. Nonetheless, we found that gait identification based on displacement amplitude versus energy phase agreed for 83.5% of walking steps and 89.9% of running steps, using 90 deg threshold for gait distinction from energy phase. It is worth noting that the reliability of any GPS-IMU-derived gait metric will depend on how closely aligned the logger is to the body CoM. Here, we placed the logger directly above the CoM position in the dorsal plane. Collar-based loggers are likely to be unsuitable for gait analysis in birds, because they exhibit pitching of the body during locomotion that would influence the phasing and amplitude of measurements from a logger located cranially to the true CoM (e.g. Andrada et al., 2014).

We identified 10,997 walking steps, 21,657 running steps, 926 walk–run transitions and 890 run–walk transitions in the 2.5 h recording of ostriches moving freely in an outdoor field. This corresponds to approximately 18 min walking and 16 min running per bird. Analysis of the stride length, stride frequency and energy phase of gait was constrained to the subset of steps that did not involve substantial turning and acceleration. Steps were excluded as turns if they involved a change in velocity heading >5.3 deg per step, or a change in velocity >0.56 m s $^{-1}$ per step. These thresholds were based on twice the interquartile range (IQR) of the data distributions. This restriction yielded 7715 of 10,997 walking steps and 18,100 of 21,657 running steps classified as ‘steady’. Excluding non-steady data did not substantially influence the observed speed

Table 1. Gait summary statistics and polynomial fits shown in Fig. 4

A. Gait summary statistics				
Gait	Speed (m s ⁻¹)	V	Energy phase (deg)	N
Walk	1.03±0.26	0.29±0.07	180±60	7715
Run	4.35±2.22	1.24±0.63	8±39	18,100
Walk–run	2.09±2.24	0.59±0.64	38±94	926
Run–walk	1.79±2.45	0.51±0.70	65±87	890
B. Second order polynomial fits: $y=a(V)^2+b(V)+c$				
	Coefficient			Adjusted R ²
	a	b	c	
Walk				
Stride length	-6.543	6.031	-0.060	0.695
Stride frequency	0.857	-0.116	0.216	0.654
Run				
Stride length	-0.126	1.500	0.499	0.959
Stride frequency	-0.038	0.256	0.313	0.844

V, relative speed; N, number of steady steps. Gait data are median and IQR.

distributions for walking and running and the distributions were not sensitive to more restrictive criteria for steadiness. All of the gait data reported here have been deposited in Dryad (see ‘Data deposition’ below; Daley et al. 2016).

On two separate days, we made similar recordings on a subset of animals without chasing (Fig. S2). The shape of the speed distribution for each gait was similar between recordings, but with varying levels of walking and running activity, and a lower maximum speed without chasing (Fig. S2). This suggests our findings are representative of the shape of the probability distributions for each gait, but not natural locomotor activity levels, which may vary for a number of reasons, including temperature, time of day and other environmental factors.

Statistics

The Matlab Curve Fitting Toolbox (Mathworks, Natick MA, USA) was used to fit 2nd-order polynomial curves relating step length and step frequency to forward velocity for the steady data. We used the robust least squares fitting option with the bi-square weights method to minimize the effect of outliers on the fitted curve. A Wilcoxon

rank sum test was used to compare the velocity distributions of walk–run and run–walk transition steps.

RESULTS

Preferred speeds of walking and running, and gait-transition speeds

We found that ostriches prefer to walk over a narrow and slow speed range and run over a broad speed range. Walking exhibited a narrow distribution centred at 1.03±0.26 m s⁻¹ (median±IQR). This corresponds to a remarkably slow relative speed [V =velocity/ \sqrt{gL}] of 0.29±0.07 (Fig. 3). The slow preferred speed of walking contrasts with the broad distribution of running speeds (Fig. 3), with a preferred running speed of 4.35±2.22 m s⁻¹ (V =1.24±0.63), and an IQR 9× greater than that of walking. The median walk–run transition occurred at 2.05±2.23 m s⁻¹ and the run–walk transition occurred at 1.77±2.28 m s⁻¹, corresponding to V of 0.58 and 0.50, respectively. The walk–run and run–walk transition distributions

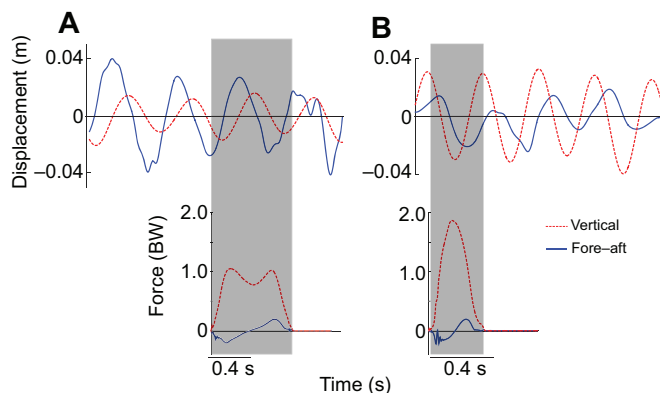


Fig. 2. Lab-based measures of fore–aft and vertical displacement with synchronized ground reaction forces, as validation of the gait detection technique used for the GPS-IMU logger data. (A) Walking at relative speed $V=0.38$ (1.34 m s⁻¹). (B) Running at $V=0.75$ (2.64 m s⁻¹). The displacements were calculated from kinematics of a marker placed on the back of the ostrich above the position of the centre of mass (CoM) in the dorsal plane, comparable to the loggers. The ground reaction force traces for a single step are shown (BW, body weight). Grey boxes indicate the duration of stance.

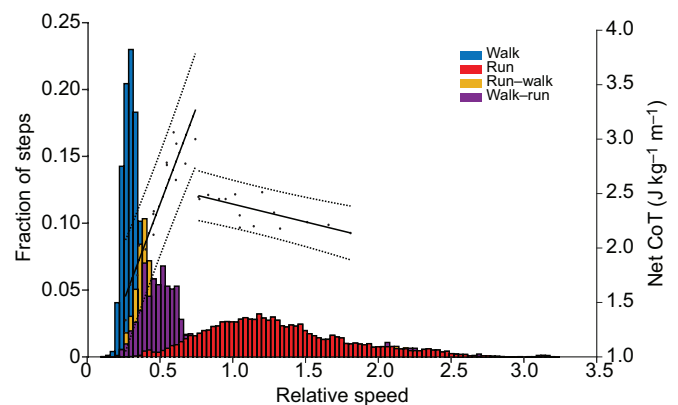


Fig. 3. Probability distributions of steps classified as walking, running, walk–run transitions and run–walk transitions of ostriches moving freely overground in an enclosed field. Data shown here were collected on a single day over a 2.5 h period (see Materials and methods). The probability distribution curves were normalized with respect to the number of steps within each gait. The summary statistics are shown in Table 1. Overlaid points and right axis show net metabolic cost of transport (CoT) for walking and running in ostriches, digitized from Watson and colleagues (2011), which included data from Fedak and Seeherman (1979). Line fit and 95% confidence intervals (solid and dotted black lines, respectively) are shown for net metabolic CoT as a function of speed and gait.

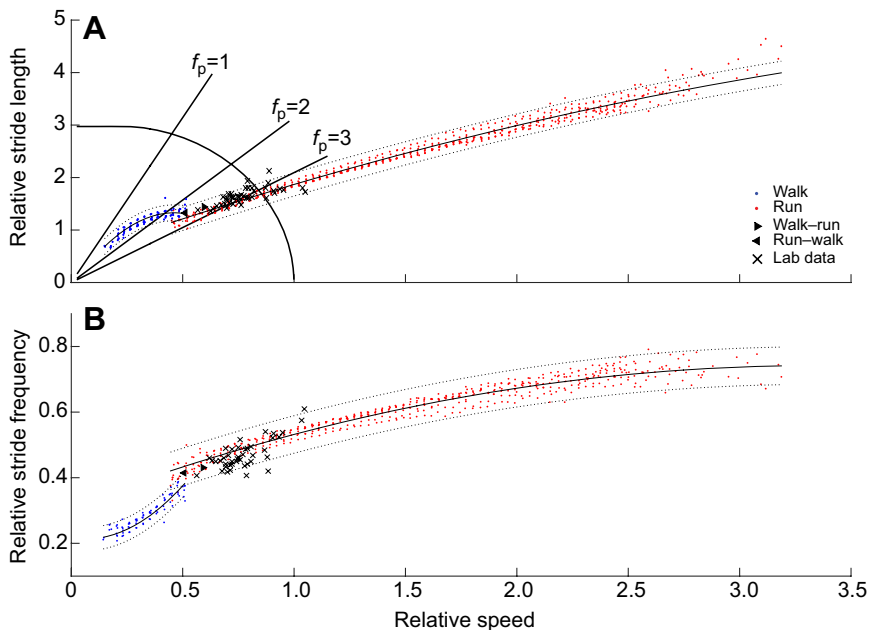


Fig. 4. Relative stride length and frequency against relative speed for the ostrich walking and running data. (A) Relative stride length. (B) Relative stride frequency. One stride is equal to two steps. Points are median values for each individual within each of 100 speed bins (bins as in Fig. 3). Curve fits with 95% confidence intervals are shown (solid and dotted black lines, respectively), fitted for all points within each gait. The median walk–run and run–walk transitions are indicated. Lab-based overground locomotion data, collected from the same individuals using high-speed video and force platforms, are overlaid (crosses; data from Birn-Jeffery et al., 2014). f_p , natural frequency of the swing leg approximated as a pendulum.

exhibited a small but consistent difference in median velocity (rank sum test, $P=7.9\times 10^{-6}$), indicating gait-transition hysteresis (Table 1, Fig. 4).

Dynamics of walking and running

An abrupt shift occurs in gait parameters between walking and running (Fig. 4), consistent with an abrupt change in locomotor dynamics at the gait transition. Near the gait transition, running uses a higher stride frequency than walking, but increases more gradually with speed thereafter (Fig. 4). An abrupt shift between walking and running also occurs in the relative phase of energy fluctuations in gravitational potential energy (E_g) and kinetic energy (E_k). As expected, walking exhibited out-of-phase fluctuations consistent with inverted pendulum dynamics, and running exhibited in-phase fluctuations consistent with mass-spring dynamics (Fig. 5). The median energy phase was 180 ± 60 deg in walking and 8 ± 39 deg in running (Table 1, Fig. 6).

DISCUSSION

Preferred walking and running speeds

Although slow, the preferred walking speed distribution of ostriches is consistent with an energetically optimal walking speed around 1.0 m s^{-1} , which correspond to speeds that allow high passive pendular energy recovery (Rubenson et al., 2004). The sharp short tail in self-selected walking speed distribution mirrors the sharp increase in net metabolic CoT of walking with speed (Fig. 3). Furthermore, these findings are consistent with the relatively low collisional losses predicted for slow walking speeds (and short step lengths) based on rigid-legged walking models (Garcia et al., 1998; Donelan et al., 2002; Ruina et al., 2005). Finally, the walking speeds measured here are consistent with field-based estimates of walking in wild ostriches (Williams et al., 1993).

The observed speed distributions for both gaits are consistent with the principle of minimizing metabolic CoT. The classic work of Hoyt and Taylor (1981) revealed that horses exhibit narrow preferred speed distributions within each gait, which correspond to the energetic optimum within U-shaped CoT curves. However, unlike horses (Hoyt and Taylor, 1981), ostriches do not appear to exhibit U-shaped curves for metabolic CoT against speed within

each gait. Instead, ostriches show a sharp linear increase in walking CoT with increasing speed, a decrease in CoT at the walk–run transition and a nearly flat (slightly decreasing) CoT curve in running (Fig. 3; Rubenson et al., 2004; Fedak and Seeherman, 1979; Watson et al., 2011). Note, however, the energetic cost of running at higher speeds ($>5.9\text{ m s}^{-1}$, $V=1.8$) is unknown, because it is challenging to get steady-state metabolic measurements from ostriches at high speeds. Nonetheless, the available metabolic data suggest that ostriches are more economical at running than walking over a broad speed range (Fig. 3). The broad distribution of running speeds used by ostriches (Fig. 3) probably reflects their low and relatively constant metabolic CoT of running.

Gait-transition speeds and hysteresis

Gait transitions occur near the optimum speed predicted by the intersection of steady-state metabolic CoT curves (Fig. 3; Rubenson et al., 2004; Watson et al., 2011), consistent with gait economy. However, this correspondence should not be interpreted as a direct causal relationship between gait transition and CoT curves. The walk–run and run–walk transition distribution of ostriches exhibited gait-transition hysteresis, and such directional effects on the preferred gait-transition speed cannot be explained by steady-state CoT curves. A similar gait-transition hysteresis has been observed in humans (Thorstensson and Roberthson, 1987; Mohler et al., 2007), and human studies suggest that neural processing and fatigue factors probably influence gait-transition speeds (Mohler et al., 2007; Segers et al., 2007). Thus, while gait transitions of ostriches occur near the energetically optimum speeds (Fig. 3), the existence of hysteresis suggests additional factors are at play in gait transition dynamics.

Dynamics of walking and running in ostriches

An abrupt change in stride length and stride frequency curves at the gait transition has not been previously observed in ostriches; however, our measures are otherwise consistent with previous studies of ostrich locomotion, including our lab-based measures (Fig. 4; Birn-Jeffery et al., 2014) and previous studies (Gatesy and Biewener, 1991; Abourachid and Renous, 2000; Rubenson et al., 2004). The difference near the gait transition might be attributed to

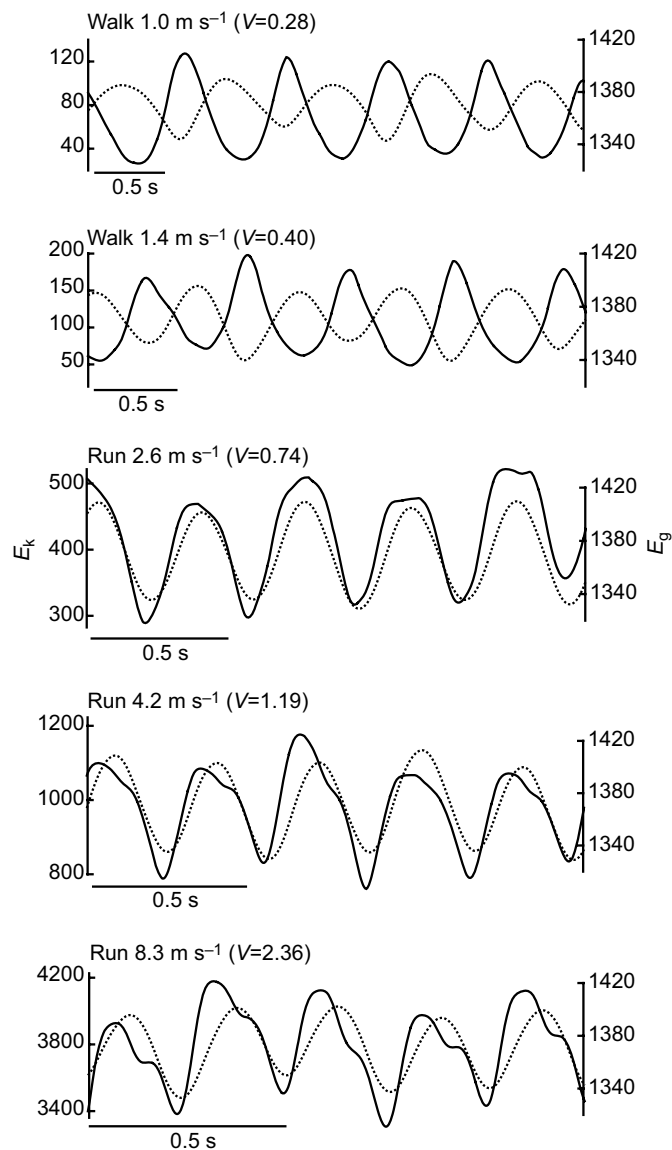


Fig. 5. Fluctuations in total kinetic energy (E_k) and gravitational potential energy (E_g) for a representative individual over a range of speeds. E_k , solid line; E_g , dotted line. Note the change in E_k axis scaling with speed, adjusted to emphasize the relative phasing between E_k and E_g . Above moderate walking speeds, E_k fluctuations are much larger in magnitude than those of E_g .

different sampling conditions among studies. Our lab-based measures spanned too narrow a speed range to resolve the gait transition (Birri-Jeffery et al., 2014). Rubenson and colleagues (2004) and Gatesy and Biewener (1991) measured locomotion at controlled speeds on a treadmill, which allows steady-state sampling, but may not reflect self-selected overground gait dynamics. Finally, Rubenson and colleagues (2004) and Abourachid and Renous (2000) used sub-adult ostriches. The normalized stride length and frequency characteristics have been found to change through ontogeny (Smith et al., 2010). Nonetheless, the overall trends of stride length and frequency with speed are remarkably consistent across studies, despite differences in data collection.

Walking exhibited out-of-phase fluctuations consistent with inverted pendulum dynamics, and running exhibited in-phase fluctuations consistent with mass-spring dynamics. However, despite consistent out-of-phase energy in walking, the capacity

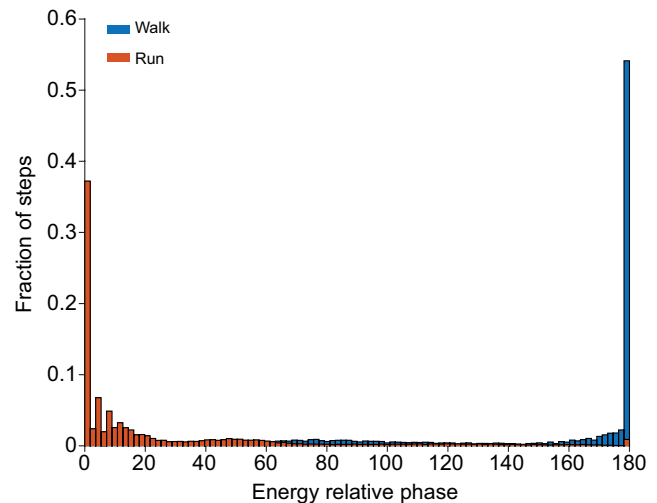


Fig. 6. Probability distribution of the relative phase of energy fluctuations for all measured walking and running steps. Data were normalized relative to the total number of steps within each gait. Summary statistics are shown in Table 1.

for inverted pendulum energy recovery diminishes rapidly with speed, because E_k fluctuations become much larger than those of E_g (Fig. 5). For example, at 1.0 m s^{-1} ($V=0.28$), E_g and E_k fluctuations are comparable in magnitude, but at 1.4 m s^{-1} ($V=0.40$), E_k fluctuations are $2.8\times$ larger (Fig. 5), indicating a maximum possible recovery of 35%. The walk–run transition occurred at $V=0.59$, a speed consistent with the previously reported transition from walking to grounded running (Rubenson et al., 2004). The absence of a distinct transition between grounded and aerial running is consistent with dynamic similarity of these gaits (Rubenson et al., 2004; S. M. O'Connor, The relative roles of dynamics and control in bipedal locomotion, PhD thesis, University of Michigan, 2009). The shift in energy phase dynamics between gaits is probably associated with increased vertical compliance resulting in a change in oscillation dynamics from walking to grounded running.

Gait-transition speeds of ostriches compared with those of humans and other animals

The compass-gait model of walking provides a useful reference for understanding how closely gait-transition speeds approach a mechanical limit necessitating an aerial phase (Alexander, 1989; Usherwood, 2005). The compass-gait model predicts maximum walking speed based on leg length and the requirement for gravity to provide sufficient centripetal force to keep the stance leg loaded in compression. Alexander (1989) identified a maximum relative walking speed of 1.0 based on mid-stance velocity resulting in foot takeoff. Usherwood (2005) extended this approach to account for the effect of step length and step frequency on maximum walking speed. Usherwood (2005) revealed that top walking speed depends on end-stance velocity, which is higher than mid-stance velocity and increases with step length. Consequently, the compass-gait boundary for top walking speed depends on the physically realizable combinations of stride length and stride frequency (Fig. 4A). Shorter steps allow faster walking (approaching 1.0 for infinitesimally short steps) but require correspondingly faster leg swing frequency. The gait-transition speeds typically reported for bipeds, between $V=0.6$ and 0.8 (e.g. Gatesy and Biewener, 1991; Hancock et al., 2007), correspond reasonably well to compass-gait model predictions after accounting for realistic leg swing

frequencies between $1.5\times$ and $2.5\times$ the natural frequency of the leg approximated as a simple pendulum (f_p ; Fig. 4A; Usherwood, 2005; Usherwood et al., 2008).

Humans walk over a broad speed range, up to speeds that fall close to the mechanical limit predicted by the compass-gait model, transitioning to a run at V near 0.7 (Usherwood, 2005; Usherwood et al., 2008), faster than the gait-transition speed of ostriches of 0.50–0.59. Additionally, the compass-gait model correctly predicts shifts in human gait-transition speeds during incline locomotion (Hubel and Usherwood, 2013). In contrast, ostrich gait transitions occur well below the maximum walking speeds predicted by the compass-gait boundary (Fig. 4A). Ostriches use unusually high step frequencies for their leg length, around $3\times f_p$ (Fig. 4A). This high step frequency suggests compass-gait boundary speeds of 0.8–0.9, considerably faster than the actual transition (Fig. 4A; Usherwood, 2005; Usherwood et al., 2008). Nonetheless, ostrich gait-transition speeds correspond well with those observed in other avian bipeds, including ducks, quail, tinamous, guinea fowl, turkeys, emus and rhea (Gatesy and Biewener, 1991; Hancock et al., 2007; Usherwood et al., 2008), suggesting the mismatch between observed and compass-gait transition speeds in ostriches reflects the limitations of this highly reduced order model rather than something unusual about ostrich gait. Still, the mismatch is informative in suggesting that other factors, such as the energetics of gait, may be more important than compass-gait mechanical limits in determining the preferred gait-transition speeds in ostriches.

One possible explanation for a relatively slower gait-transition speed in ostriches compared with humans could be that the avian hip does not contribute substantially to forward progression, especially at slow speeds (Gatesy, 1999; Abourachid and Renous, 2000; Smith et al., 2010; Rubenson et al., 2011), so the ‘effective leg’ might be approximated to originate at the knee. However, this potential decrease in effective leg length does not fully explain the relatively slow walking of the ostrich. For the ostrich to transition to running at a similar V to humans, the effective leg length would need to be 0.82 m rather than 1.25 m, putting the virtual leg origin in an unrealistic position 35% distal to the hip, well below the knee and the vertical position of the body CoM (Rubenson et al., 2011). Thus, a shorter effective leg length in walking ostriches does not adequately explain their relatively slower gait-transition speed compared with that of humans.

An alternative explanation for a difference in gait-transition speeds between ostriches and humans might relate to the relative costs of walking and running. While humans and ostriches have similar costs of walking for their body size, ostriches are relatively economical runners, whereas humans are relatively costly runners (Rubenson et al., 2007). Ostrich limb anatomy exhibits many specialized cursorial features, including elongated, fused and reduced distal elements and well-developed distal ligaments and tendons to enhance elastic energy cycling and allow high step frequencies to be achieved relatively cheaply (Smith et al., 2006; Schaller et al., 2009; Rubenson et al., 2011; Smith and Wilson, 2013). The slow transition to running and the broad distribution of self-selected running speeds exhibited by ostriches probably reflects their exceptionally well-specialized distal limb elasticity, thanks to a heritage of bipedal cursoriality extending back to theropod dinosaurs.

Maximum running speeds in ostriches

We measured maximal running speeds around 11.3 m s^{-1} (25.3 mph, $V=3.2$; Fig. 4). Although this is faster than has been measured in lab-based studies (Abourachid and Renous, 2000; Rubenson et al., 2004; Fedak and Seeherman, 1979; Watson et al.,

2011), it may not reflect maximum sustainable speed of ostriches. Alexander and colleagues (1979) report maximum speed between 12 and 17 m s^{-1} (26.8–38.0 mph), depending on whether the video footage or vehicle odometer, respectively, was used to estimate velocity. They reported maximum stride frequency of 2.3 Hz, slightly higher than the maximum of 1.95 Hz measured here, suggesting that the ostriches recorded by Alexander and colleagues (1979) were travelling faster. To our knowledge, reliable direct measurements of maximum running speed of ostriches do not exist, despite widespread popular reports of maximum speeds reaching $20\text{--}27\text{ m s}^{-1}$ (45–60 mph). Recent GPS-IMU tracking has allowed direct confirmation of the remarkable top speeds of hunting wild cheetahs (25.9 m s^{-1} , 59 mph; Wilson et al., 2013). It would be useful to similarly track wild ostriches over extended periods to better relate lab-based measures of locomotor dynamics to those used during foraging, migration and predator escape in the wild.

Conclusions

Ostriches prefer to walk very slowly, with a narrow distribution consistent with minimizing CoT according to rigid-legged walking models. When running, ostriches use a broad speed distribution, consistent with their relatively economical and flat curve for the CoT of running. The self-selected gait-transition speeds in ostriches are more consistent with minimizing of metabolic CoT than with a mechanical limit necessitating an aerial phase. Overall, our findings support the validity of lab-based measures of gait mechanics and energetics for predicting self-selected locomotor behaviour in natural terrain. However, ostriches, like humans, exhibit a gait-transition hysteresis that cannot be explained by steady-state locomotor dynamics and energetics.

Acknowledgements

We thank Alan Wilson for use of the GPS-IMU loggers, Aleksandra Birn-Jeffery and Rebecca Fisher for their contributions to animal care and training, Jim Usherwood for helpful discussions and providing the compass gait model predictions shown in Fig. 4, and David Lee for discussions of the differences between birds and humans. Alan Wilson, Tatjana Hubel and many others in the Structure and Motion Lab also provided useful discussion and feedback.

Competing interests

The authors declare no competing or financial interests.

Author contributions

M.A.D. and A.J.C. conceived and designed the study, A.J.C. and G.S.N. performed the experiments, G.S.N., J.H. and M.A.D. analysed the data, J.H. and M.A.D. wrote the paper, and M.A.D. supervised the research.

Funding

This work was supported grant (BB/H005838/1) to M.A.D. from the Biotechnology and Biological Sciences Research Council (BBSRC).

Data availability

Data are available from the Dryad Digital Repository: <http://dx.doi.org/10.5061/dryad.h846r>.

Supplementary information

Supplementary information available online at <http://jeb.biologists.org/lookup/doi/10.1242/jeb.142588.supplemental>

References

- Abourachid, A. and Renous, S. (2000). Bipedal locomotion in ratites (Paleognathiform): examples of cursorial birds. *Ibis* **142**, 538–549.
- Alexander, R. M. (1989). Optimization and gaits in the locomotion of vertebrates. *Physiol. Rev.* **69**, 1199–1227.
- Alexander, R. M. (1992). A model of bipedal locomotion on compliant legs. *Philos. Trans. R. Soc. B Biol. Sci.* **338**, 189–198.
- Alexander, R. M. (2004). Bipedal animals, and their differences from humans. *J. Anat.* **204**, 321–330.

- Alexander, R. M., Maloiy, G. M. O., Njau, R. and Jayes, A. S. (1979). Mechanics of running of the ostrich (*Struthio camelus*). *J. Zool.* **187**, 169-178.
- Andrada, E., Nyakatura, J., Müller, R., Rode, C. and Blickhan, R. (2012). Grounded running: an overlooked strategy for robots. In *Autonomous Mobile Systems* (ed. P. Levi, O. Zweigle, K. Häußermann and B. Eckstein), pp. 79-87. Berlin; Heidelberg: Springer.
- Andrada, E., Rode, C., Sutedja, Y., Nyakatura, J. A. and Blickhan, R. (2014). Trunk orientation causes asymmetries in leg function in small bird terrestrial locomotion. *Proc. R. Soc. Lond. B Biol. Sci.* **281**, 20141405.
- Birn-Jeffery, A. V. and Daley, M. A. (2012). Birds achieve high robustness in uneven terrain through active control of landing conditions. *J. Exp. Biol.* **215**, 2117-2127.
- Birn-Jeffery, A. V., Hubicki, C. M., Blum, Y., Renjewski, D., Hurst, J. W. and Daley, M. A. (2014). Don't break a leg: running birds from quail to ostrich prioritise leg safety and economy on uneven terrain. *J. Exp. Biol.* **217**, 3786-3796.
- Cavagna, G. A., Heglund, N. C. and Taylor, C. R. (1977). Mechanical work in terrestrial locomotion: two basic mechanisms for minimizing energy expenditure. *Am. J. Physiol. Regul. Integr. Comp. Physiol.* **233**, R243-R261.
- Cotton, S., Olaru, I. M. C., Bellman, M., Van der Ven, T., Godowski, J. and Pratt, J. (2012). Fastrunner: A fast, efficient and robust bipedal robot. concept and planar simulation. In IEEE International Conference on Robotics and Automation (ICRA) 2012, 2358-2364.
- Daley, M. A., Channon, A. J., Nolan, G. S. and Hall, J. (2016). Data from: Preferred gait and walk-run transition speeds in ostriches measured using GPS-IMU sensors. *Dryad Digital Repository*. <http://dx.doi.org/10.5061/dryad.h846r>
- Donelan, J. M., Kram, R. and Kuo, A. D. (2002). Mechanical work for step-to-step transitions is a major determinant of the metabolic cost of human walking. *J. Exp. Biol.* **205**, 3717-3727.
- Fedak, M. A. and Seeherman, H. J. (1979). Reappraisal of energetics of locomotion shows identical cost in bipeds and quadrupeds including ostrich and horse. *Nature* **282**, 713-716.
- Garcia, M., Chatterjee, A., Ruina, A. and Coleman, M. (1998). The simplest walking model: stability, complexity, and scaling. *J. Biomech. Eng.* **120**, 281-288.
- Gatesy, S. M. (1999). Guineafowl hind limb function. I: Cineradiographic analysis and speed effects. *J. Morphol.* **240**, 115-125.
- Gatesy, S. M. and Biewener, A. A. (1991). Bipedal locomotion: effects of speed, size and limb posture in birds and humans. *J. Zool.* **224**, 127-147.
- Geyer, H., Seyfarth, A. and Blickhan, R. (2006). Compliant leg behaviour explains basic dynamics of walking and running. *Proc. R. Soc. Lond. B Biol. Sci.* **273**, 2861-2867.
- Hancock, J. A., Stevens, N. J. and Biknevicius, A. R. (2007). Whole-body mechanics and kinematics of terrestrial locomotion in the elegant-crested tinamou *Eudromia elegans*. *Ibis* **149**, 605-614.
- Hoyt, D. F. and Taylor, C. R. (1981). Gait and the energetics of locomotion in horses. *Nature* **292**, 239-240.
- Hubel, T. Y. and Usherwood, J. R. (2013). Vaulting mechanics successfully predict decrease in walk-run transition speed with incline. *Biol. Lett.* **9**, 20121121.
- Hubel, T. Y., Myatt, J. P., Jordan, N. R., Dewhirst, O. P., McNutt, J. W. and Wilson, A. M. (2016). Energy cost and return for hunting in African wild dogs and cheetahs. *Nat. Commun.* **7**, 11034.
- Mohler, B. J., Thompson, W. B., Creem-Regehr, S. H., Pick, H. L., Jr and Warren, W. H. Jr. (2007). Visual flow influences gait transition speed and preferred walking speed. *Exp. Brain Res.* **181**, 221-228.
- Rubenson, J., Heliams, D. B., Lloyd, D. G. and Fournier, P. A. (2004). Gait selection in the ostrich: mechanical and metabolic characteristics of walking and running with and without an aerial phase. *Proc. R. Soc. Lond. B Biol. Sci.* **271**, 1091-1099.
- Rubenson, J., Heliams, D. B., Maloney, S. K., Withers, P. C., Lloyd, D. G. and Fournier, P. A. (2007). Reappraisal of the comparative cost of human locomotion using gait-specific allometric analyses. *J. Exp. Biol.* **210**, 3513-3524.
- Rubenson, J., Lloyd, D. G., Heliams, D. B., Besier, T. F. and Fournier, P. A. (2011). Adaptations for economical bipedal running: the effect of limb structure on three-dimensional joint mechanics. *J. R. Soc. Interface* **8**, 830-847.
- Ruina, A., Bertram, J. E. A. and Srinivasan, M. (2005). A collisional model of the energetic cost of support work qualitatively explains leg sequencing in walking and galloping, pseudo-elastic leg behavior in running and the walk-to-run transition. *J. Theor. Biol.* **237**, 170-192.
- Schaller, N. U., Herkner, B., Villa, R. and Aerts, P. (2009). The intertarsal joint of the ostrich (*Struthio camelus*): anatomical examination and function of passive structures in locomotion. *J. Anat.* **214**, 830-847.
- Segers, V., Lenoir, M., Aerts, P. and De Clercq, D. (2007). Influence of M. tibialis anterior fatigue on the walk-to-run and run-to-walk transition in non-steady state locomotion. *Gait Posture* **25**, 639-647.
- Smith, N. C. and Wilson, A. M. (2013). Mechanical and energetic scaling relationships of running gait through ontogeny in the ostrich (*Struthio camelus*). *J. Exp. Biol.* **216**, 841-849.
- Smith, N. C., Wilson, A. M., Jespers, K. J. and Payne, R. C. (2006). Muscle architecture and functional anatomy of the pelvic limb of the ostrich (*Struthio camelus*). *J. Anat.* **209**, 765-779.
- Smith, N. C., Jespers, K. J. and Wilson, A. M. (2010). Ontogenetic scaling of locomotor kinetics and kinematics of the ostrich (*Struthio camelus*). *J. Exp. Biol.* **213**, 1347-1355.
- Srinivasan, M. (2011). Fifteen observations on the structure of energy-minimizing gaits in many simple biped models. *J. R. Soc. Interface* **8**, 74-98.
- Srinivasan, M. and Ruina, A. (2006). Computer optimization of a minimal biped model discovers walking and running. *Nature* **439**, 72-75.
- Thorstensson, A. and Roberthson, H. (1987). Adaptations to changing speed in human locomotion: speed of transition between walking and running. *Acta Physiol. Scand* **131**, 211-214.
- Usherwood, J. R. (2005). Why not walk faster? *Biol. Lett.* **1**, 338-341.
- Usherwood, J. R. and Hubel, T. Y. (2012). Energetically optimal running requires torques about the centre of mass. *J. R. Soc. Interface* **9**, 2011-2015.
- Usherwood, J. R., Szymanek, K. L. and Daley, M. A. (2008). Compass gait mechanics account for top walking speeds in ducks and humans. *J. Exp. Biol.* **211**, 3744-3749.
- Watson, R. R., Rubenson, J., Coder, L., Hoyt, D. F., Propert, M. W. G. and Marsh, R. L. (2011). Gait-specific energetics contributes to economical walking and running in emus and ostriches. *Proc. R. Soc. Lond. B Biol. Sci.* **278**, 2040-2046.
- Williams, J. B., Siegfried, W. R., Milton, S. J., Adams, N. J., Dean, W. R. J., du Plessis, M. A. and Jackson, S. (1993). Field metabolism, water requirements, and foraging behavior of wild ostriches in the Namib. *Ecology* **74**, 390-404.
- Wilson, A. M., Lowe, J. C., Roskilly, K., Hudson, P. E., Golabek, K. A. and McNutt, J. W. (2013). Locomotion dynamics of hunting in wild cheetahs. *Nature* **498**, 185-189.